ICIC Express Letters
Part B: Applications
Volume **7**, Number **1**, January **2016**

ICIC International ©2016 ISSN 2185-2766
pp. **85–90**

MULTIAPERTURE SUPER RESOLUTION ALGORITHM BASED ON THE SENSOR ARRAY

Haitian Zhai, Hui Li and Yang Zhao

School of Electronics and Information
Northwestern Polytechnical University
No. 127, West Youyi Road, Xi'an 710072, P. R. China
haitian_1988@mail.nwpu.edu.cn

Received June 2015; accepted September 2015

Abstract. *Recent advances employing the image sensor array include synthesizing novel views from the captured images, increasing field-of-view, and implementation in the infrared. This paper presents a system that captures a sequence of low resolution images from an image sensor array to construct a more detailed high resolution image. The proposed system is able to increase the angular resolution beyond the Nyquist limit. Synthetic and non-synthetic images are used to evaluate the performance of the proposed system. The results show that robust recovery of high resolution images can be obtained by our system. The proposed system can be employed to a wide area of image processing applications such as remote sensing, robotic vision, and infrared image enhancement.*
Keywords: Sensor array, Super resolution, Response function, HR reconstruction

1. **Introduction.** High-resolution (HR) imaging systems are constantly required in many application fields, such as video surveillance [1] and remote sensing [2]. However, due to the limitation of hardware and imaging environment, in some cases, it is difficult to obtain images at a desired resolution level. To increase the resolution, there is a fundamental limit on the smallest size of the focus spot one can reach with conventional optics. The limit originates from the light diffraction, which is around one-half wavelength of the light $\sim \lambda/2$. In the last few decades, efforts have been made to overcome the diffraction limit. One promising method called super-resolution (SR) [3-5] has been introduced to recover the details of an image from a sequence of low resolution (LR) images.

In traditional SR methods, multiple scenes are always obtained from one camera with several captures; however, multiple cameras located in different positions, such as sensor arrays [6], can also acquire multiple frames. The use of an array of image sensor, LR imagers enable a significant reduction in the depth of the imaging system by a factor equal to the number of lenslets used across the detector array. Many camera arrays have been proposed to capture images simultaneously from multiple viewpoints. Recent advances employing multiple imaging sensors include improvements in signal processing, implementation in the infrared, and increasing field of view. However, none of these deal the angular resolution limit due to use of a single-detector array. Here we introduce a multiaperture imaging system implemented using an image sensor array.

This paper presents an efficient way to enhance image resolution using our image sensor array. We show that the proposed system performs well for different noise levels. The rest of the paper is organized as follows. In Section 2, we introduced our system model by discussing the response function of the imaging system. In Section 3, both synthetic and non-synthetic images are used to evaluate the performance of the proposed system. Finally, conclusions from this study are provided in Section 4.

2. **Response Function and the Sensor Array.** The response function [7], which contains useful information about apparent sampling artifacts in the image, describes the spatial frequency transfer function of an imaging system. Similar to the approach utilized in nonsampled imaging system, the response of the sampled system can be derived by considering the system response as a point source. We separate the whole image formation process into two steps including the pre-sampling step and sampling components step for most sampled imaging systems. H_{opt} is denoted as optical transfer function and H_{pix} is denoted as pixel transfer function, both of which describe the pre-sampling component accounting for the spatial frequency filtering due to the finite size of the sensors in Fourier domain.

$$H_{pix}(f_s) = \mathrm{sinc}(mf_s) = \frac{\sin(\pi m f_s)}{\pi m f_s} \tag{1}$$

where f_s is the spatial frequency and m is the full width of the pixel.

The sampling component of the response function can be represented by a comb of delta functions with sampling frequency $f_p = 1/X$, where X is the interval between sampling points, which yields,

$$\Lambda(f_s) = \sum_n \delta(f_s - nf_p) \tag{2}$$

We multiply the three transfer functions H_{opt}, H_{pix}, and Λ in the frequency domain to yield a combined response function for the imaging and sampling process,

$$R(f_s, \phi) = H_{pix}(f_s) \sum_n (f_s - nf_p)\, e^{(in\phi)} \tag{3}$$

We can observe from (3) that the sampling process replicates H_{opt} at nf_p. All of the replicated spectra are multiplied by H_{pix} centered at $f_s = 0$ to yield the final spectrum. Due to the fact that each spectrum varies in phase from the neighbor spectrum by the sample phase increment ϕ, the sampled response function $R(f_s, \phi)$ will depend on the relative position of the sampling points and the pre-sampled point-spread function (PSF). There are two contributions of the mathematical derivation of the sampling process to $R(f_s, \phi)$: a spurious response and a transfer function. The spurious response component is determined by multiplying H_{pix} by all the spectra except the one located at $n = 0$, and is conditioned by f_p and ϕ. The transfer function is independent of the sampling interval and it is simply the product of the H_{opt} and H_{pix}. The overlapped region between the baseband spectrum and the spurious response varies with the sampling frequency and is

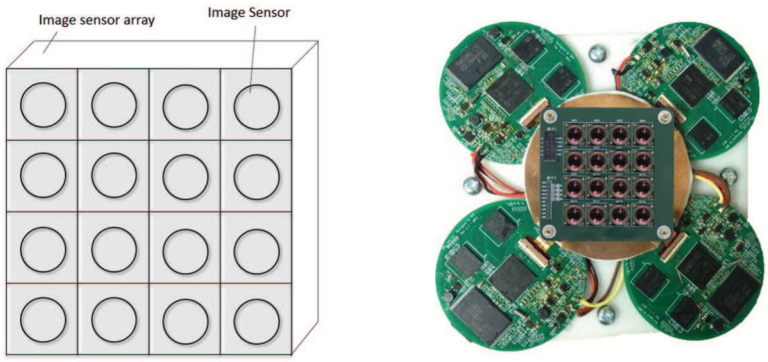

(a) (b)

FIGURE 1. (a) Image sensor array schematic. (b) Prototype of the proposed model. The array consists of 16 image sensors, and each of the imager has a 60 degree FOV. These sensors are independent with each other forming almost overlapped LR images.

the main indicator of the magnitude of the sampling artifact in the image. If the sampling frequency is small, the spurious response will totally corrupt the baseband.

Since none of the existing camera arrays would have both the functioning and positioning flexibility that our system required. Therefore, we build our imaging sensor arrays ourselves. Shown in Figure 1 is the sensor array we used in our system. We incorporate existing technology as much as possible to simplify hardwares our system needed for operation. The choice of the image sensor is a critical decision since it determines the performance of the system as well as the cost. 16 inexpensive sensors and lenses with a common field of view which is around 60° are used, and these sensors form an array of discrete and independent, almost overlapped LR images.

HR reconstruction makes use of information obtained from LR images recorded in these sensors to produce an HR image. Useful information from all LR images is reached by calculating subpixel displacements so that the sampling displacements δ_k must vary among low resolution sensors. For an $N \times N$ image sensor array, the ideal displacements between adjacent LR sensors are $\Delta d_k = d_{k+1} - d_k = \pm 1/(Nf_s)$. So we can get the sampling offset which is

$$\Delta d = f\frac{D}{R} \tag{4}$$

where R is the range of the object, and f is the focal length of lenslets spaced on an array of period D.

3. **Main Results.** We have conducted a number of experiments with two types of data including synthetic images and real images obtained using our model to test the performance of the proposed sytem. For the synthetic experiment, we first calculate the pixel displacement errors and rotation errors using feature based subpixel registration algorithm. Then for the performance evaluation, peak signal to noise ratio and structural similarity index measure (SSIM) with different noise levels are calculated. For the real data, we reconstruct the HR image using a sequence of LR images obtained using our system and we also tested how well our system performs under various numbers of frames.

The experimental results are first presented using synthetic images. 12 synthetic LR images have been generated from an HR image shown in Figure 2(a). The sequence of LR frames of 60×60 pixels from the original image is generated as following steps. First, we convolve the HR image with a Gaussian blur kernel to simulate the effect of camera PSF. Then, the resulting image was downsampled by the factor of 2 in horizontal and vertical direction. The same approach with different warping operations was used to produce 12 LR images.

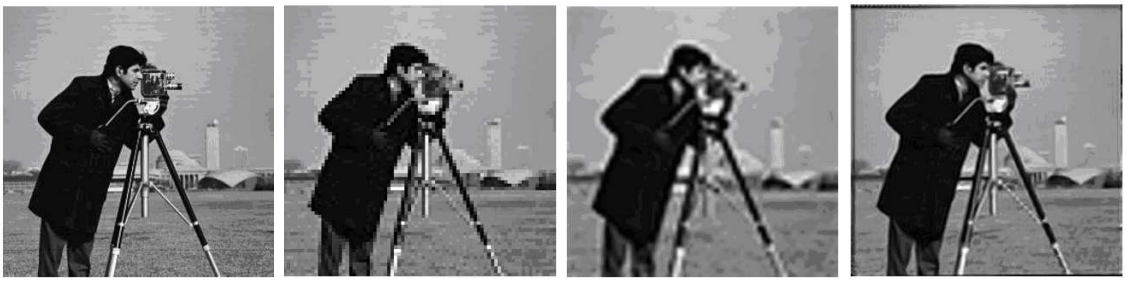

(a) (b) (c) (d)

FIGURE 2. An example of synthetic HR reconstruction using proposed system: (a) original HR image, (b) LR image enlarged with nearest neighbor interpolation, (c) LR image enlarged with bicubic interpolation, (d) reconstructed HR image

LR images are further degraded by additive white noise with noise power 10 dB, 15 dB, 20 dB, and 30 dB. Figure 2(b) shows one of 12 synthetic LR images. HR images obtained by bicubic interpolation and super resolution using our system are shown in Figures 2(c) and 2(d), respectively. We see from Figure 2 that the quality of the reconstructed image by the proposed mechanism is better than traditional bicubic interpolation which means our system can actually improve the image quality.

For the performance evaluation between the original HR and SR reconstructed images, the quality of the reconstructed HR images has been quantitatively measured in terms of the PSNR, which measures denoising effectiveness. We then test the performance of our system under various noise levels. Figure 3(a) shows the PSNR at different noise levels with different amounts of frames. The high value of the PSNR demonstrates the effectiveness of the SR scheme. Our mechanism is able to produce fine details and recover major image structure even under heavy noise. However, traditional interpolation methods such as nearest neighbor or bicubic interpolation can only increase the amount of pixels without reconstructing the details of the image or denoising. Note that the performance drops as the noise level increases are consistent with our theoretical analysis.

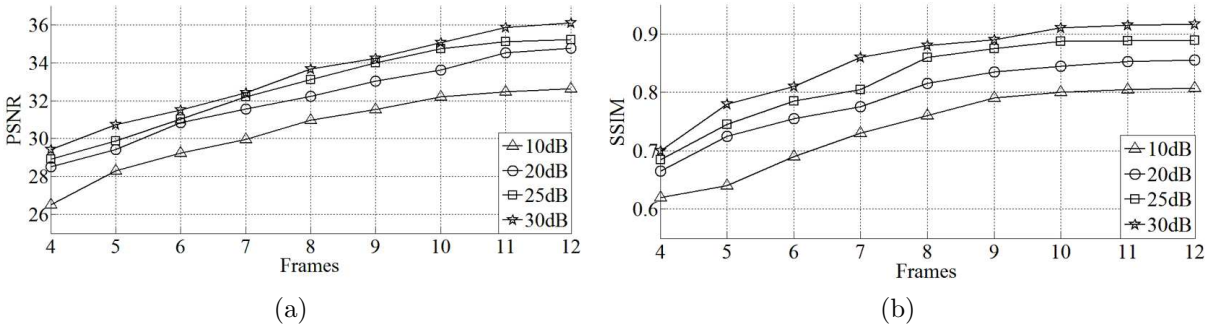

(a) (b)

FIGURE 3. (a) PSNR at different noise levels, (b) SSIM at different noise levels

To evaluate the spatial-temporal inconsistency of the reconstructed HR image, structural similarity index measure (SSIM), which measures visual similarity between images, is also used to evaluate the performance of our system. Figure 3(b) shows the SSIM value at different noise levels with different amounts of frames. As we can see in the figure, when the power of additional noise increases, the SSIM value of each restored SR images becomes worse. The result is consistent with PSNR which indicates that our system is able to recover details even under very heavy noise which means the proposed method is robust to the noise.

In the non-synthetic experiment, we use a dataset containing 16 frames shown in Figure 4(a) to illustrate the effectiveness of proposed mechanism. In order to present the performance of proposed system more comprehensively, we amplify the same region for the frame before super resolution shown in Figure 4(b) and the frame after super resolution shown in Figure 4(c). The rectangular regions in Figures 4(b) and 4(c) are enlarged and shown in the associated images for closer observation. For the LR frame, it is stretched using bicubic interpolation to the same size as the HR frame. For SR algorithm, the reconstructed image should preserve the edges, texture, contrast invariance and geometric invariance of the input image. Through the comparison of the LR image and the reconstructed image shows that our method provides obvious good subjective visual quality with rich textures and sharp edges, and the increase in resolution and image quality is evident. Either the increased effective sampling frequency, or the diffraction limit of individual sensor limits the achievable increase in resolution. In practice, the resolution increase is also determined by optical distortion, sub-pixel registration accuracy, and degree of redundancy.

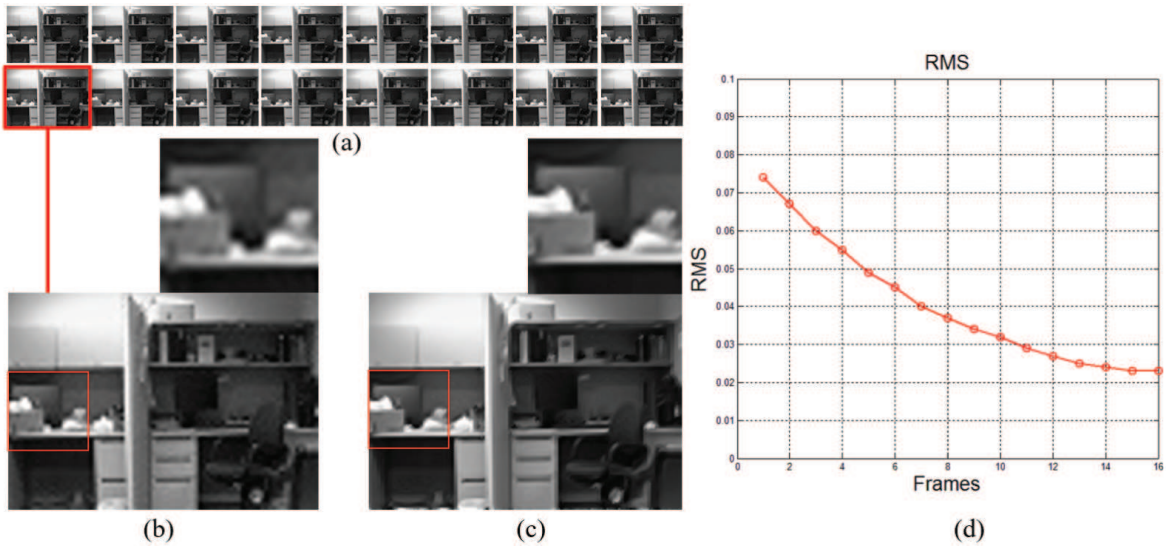

FIGURE 4. An example of non-synthetic HR reconstruction using proposed system: (a) 16 LR frames obtained by our system, (b) one of 16 LR images enlarged with bicubic interpolation, (c) reconstructed HR image using proposed SR algorithm, (d) RMS with different number of frames

We have also tested the performance of our system under various numbers of frames. Figure 4(d) shows the root-mean-square error (RMSE) between the image reconstructed using 16 frames and the image reconstructed using a subset of 16 frames is utilized to explore the relationship between image quality and the number of frames is used. As can be seen from the figure, the magnitude of aliasing artifacts is clearly reduced with increasing number of frames.

4. **Conclusions.** A novel image sensor array that captures a sequence of LR images to construct a more detailed HR image is presented in this paper. The proposed model can increase the image resolution obtained by a camera array beyond the Nyquist limit. The results of the experiment with synthetic and non-synthetic images show that proposed model is able to recover the image at different noise levels even if the noise is very high. The proposed system can be employed to a wide area of image processing applications such as remote sensing, robotic vision, and infrared image enhancement.

Acknowledgment. This work is partially supported by National Natural Science Foundation of China (Grant No. 61171155 and No. 61571364), and Doctorate Foundation of Northwestern Polytechnical University (No. CX201316). The authors also gratefully acknowledge the helpful comments and suggestions of the reviewers, which have improved the presentation.

REFERENCES

[1] S. C. Park, M. K. Park and M. G. Kang, Super-resolution image reconstruction: A technical overview, *IEEE Signal Processing Magazine*, vol.20, no.3, pp.21-36, 2003.

[2] M. G. Hu, J. F. Wang and Y. Ge, Super-resolution reconstruction of remote sensing images using multifractal analysis, *Sensors*, vol.9, pp.8669-8683, 2009.

[3] H. K. Chen, C. H. Chen and S. J. Wang, A fast and robust map-based superresolution reconstruction method using cdhs and block-wise motion vector selection, *International Journal of Innovative Computing, Information and Control*, vol.6, no.7, pp.3105-3120, 2010.

[4] J. Guan, J. Yang, Y. Huang and W. Li, A maximum likelihood-based angular super-resolution algorithm in gaussian noise for real-beam scanning radar, *ICIC Express Letters*, vol.9, no.6, pp.1707-1712, 2015.

[5] E. M. Hung, R. L. De Queiroz, F. Brandi, K. F. De Oliveira and D. Mukherjee, Video super-resolution using codebooks derived from key-frames, *IEEE Trans. Circuits and Systems for Video Technology*, vol.22, pp.1321-1331, 2012.

[6] S. Z. M. Muji, R. A. Rahim, M. H. F. Rahiman, S. Sahlan, M. F. A. Shaib, M. Jaysuman and E. J. Mohamad, Optical tomography: A review on sensor array, projection arrangement and image reconstruction algorithm, *International Journal of Innovative Computing, Information and Control*, vol.7, no.7, pp.3839-3856, 2011.

[7] G. Muyo, A. Singh, M. Andersson, D. Huckridge, A. Wood and A. R. Harvey, Infrared imaging with a wavefront-coded singlet lens, *Optics Express*, pp.21118-21123, 2009.